NANO MICRO small

Supporting Information

for *Small,* DOI: 10.1002/smll.202200177

Investigating the Role of Surface Roughness and Defects on EC Breakdown, as a Precursor to SEI Formation in Hard Carbon Sodium-Ion Battery Anodes

Emilia Olsson, Jonathon Cottom, Hande Alptekin, Heather Au, Maria Crespo-Ribadeneyra, Maria-Magdalena Titirici, and Qiong Cai**

Supporting Information for

Investigating the role of surface roughness and defects on EC breakdown, as a precursor to SEI formation in hard carbon sodium-ion battery anodes.

Emilia Olsson [a,b,c], Jonathon Cottom[d,e], Hande Alptekin[b,f], Heather Au[b], Maria Crespo-Ribadeneyra[b], Maria-Magdalena Titirici[b], and Qiong Cai[a,*]

[a] Department of Chemical and Process Engineering, University of Surrey, Guildford, GU2 7XH, United Kingdom

[b] Department of Chemical Engineering, Imperial College London, SW7 2AZ, London, United Kingdom

[c] Current Address: Advanced Research Centre for NanoLithography, Science Park 106, 1098 XG, Amsterdam, the Netherlands, and Institute of Physics, University of Amsterdam, Science Park 904, 1098 XH, Amsterdam, the Netherlands.

[d] Department of Physics and Astronomy, University College London, London, WC1E 6BT, United Kingdom.

[e] Current Address: Leiden Institute of Chemistry, University of Leiden, 2333 CC Leiden, the Netherlands

[f] Department of Materials, Imperial College London, Exhibition Road, London SW7 2AZ, UK

[*]Corresponding author. Tel: +44(0)1483686561 E-mail: q.cai@surrey.ac.uk (Qiong Cai)

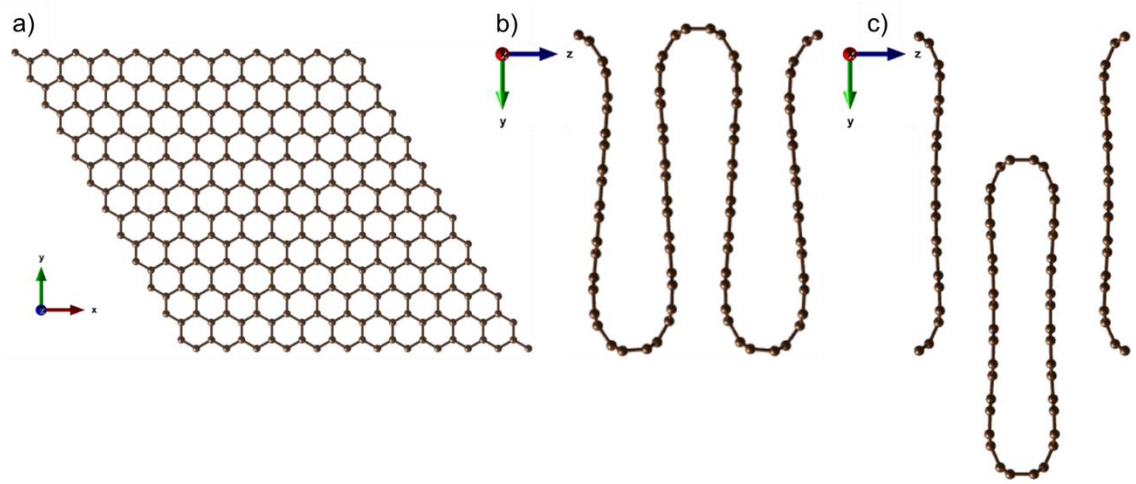

Figure S1. Simulation models used for a) basal plane, b) abrupt surface, and c) rough model. All models are 3D periodic, with a 25 Å vacuum gap in a) the z-direction (blue arrow axis), and b), c) in the y-direction (green arrow axis). Brown spheres are carbon atoms.

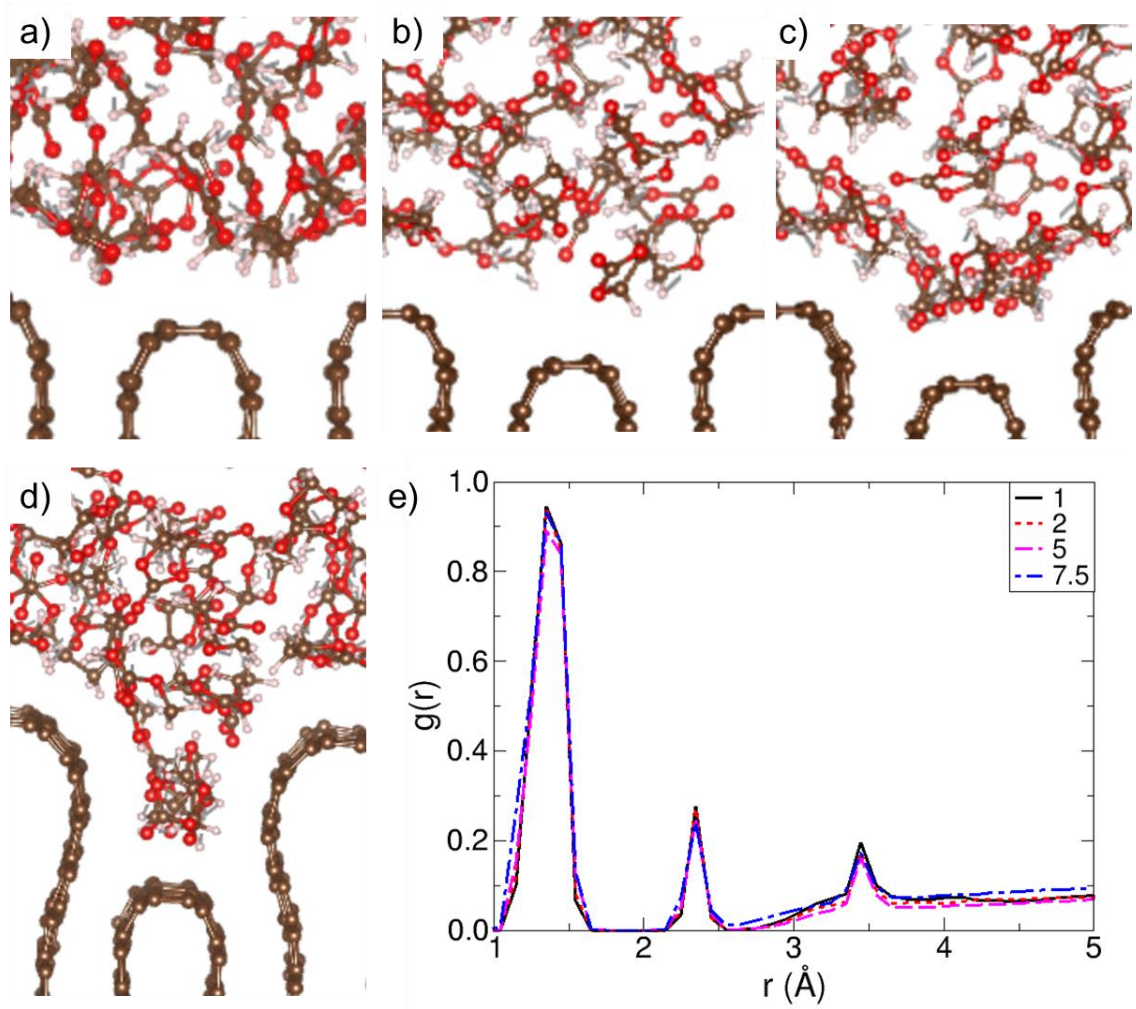

Figure S2. Snapshots of AIMD simulations for models with troughs of a) 1 Å, b) 2 Å, c) 5 Å, and d) 7.5 Å. e) shows the C-O pair correlation function (g(r)) for the models in a-d. Brown spheres are carbon atoms, red oxygen, and white hydrogen.

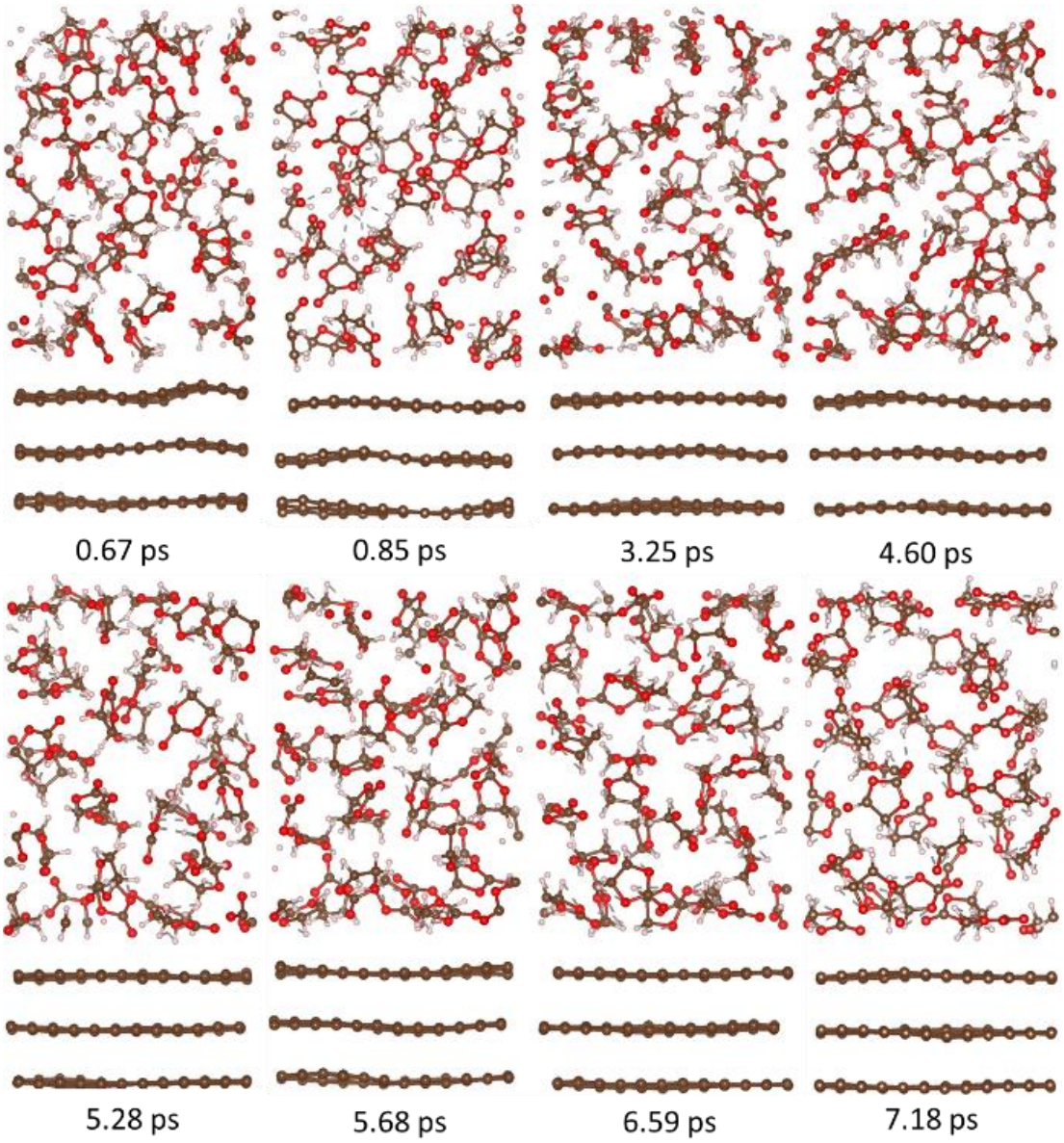

Figure S3. Snapshots of the EC basal plane AIMD simulations showing the rumpling of the graphene sheets. Brown spheres are carbon atoms, red oxygen, and white hydrogen.

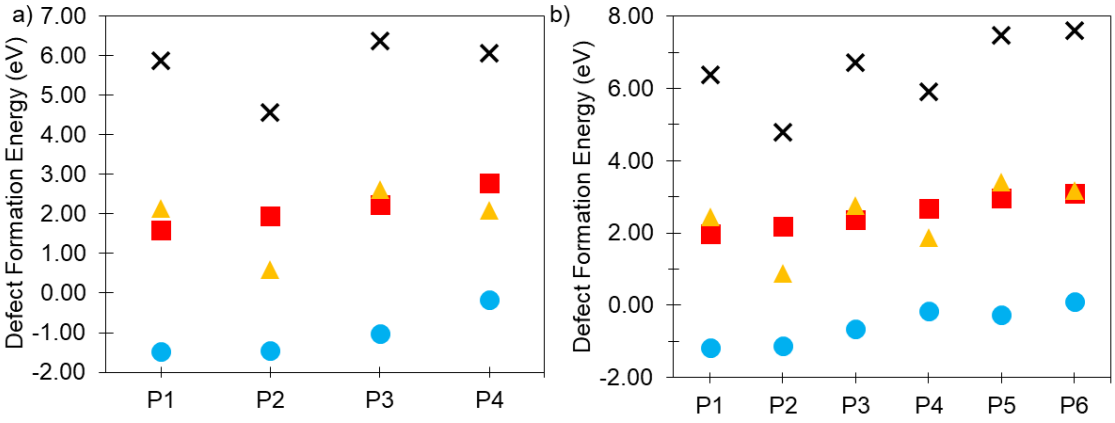

Figure S4. Defect formation energies for $2O_C$ (blue circles), O_C (red squares), O_CV_C (yellow triangles), and V_C (black crosses) in a) 2 Å, and b) 5 Å rough models.

For the figures on the next few pages the figure captions are given on the next consecutive page.


a)
b)
c)
d)
e)
f)
g)
h)
i)
j)
k)
l)
m)
n)
o)
p)
q)
r)
s)
t)
u)
v)
w)
x)
y)
z)
å)
ä)

Figure S5. Zoomed in view of optimised structure for the rough models with EC at defect sites (nomeclature for defect sites is given in Figure 1b in the main paper). Row one shows EC at site P1 with a) $2O_C$ defect, b) O_C defect, c) O_CV_C defect, and d) V_C defect. Row two shows EC at site P2 with e) $2O_C$ defect, f) O_C defect, g) O_CV_C defect, and h) V_C defect. Row three shows EC at site P3 with i) $2O_C$ defect, j) O_C defect, k) O_CV_C defect, and l) V_C defect. Row four shows EC at site P4 with m) $2O_C$ defect, n) O_C defect, o) O_CV_C defect, and p) V_C defect. Row five shows EC at site P5 with q) $2O_C$ defect, r) O_C defect, s) O_CV_C defect, and t) V_C defect. Row six shows EC at site P6 with u) $2O_C$ defect, v) O_C defect, w) O_CV_C defect, and x) V_C defect. Row seven shows EC at site P7 with y) $2O_C$ defect, z) O_C defect, å) O_CV_C defect, and ä) V_C defect. Brown spheres are carbon atoms, red oxygen, and white hydrogen.

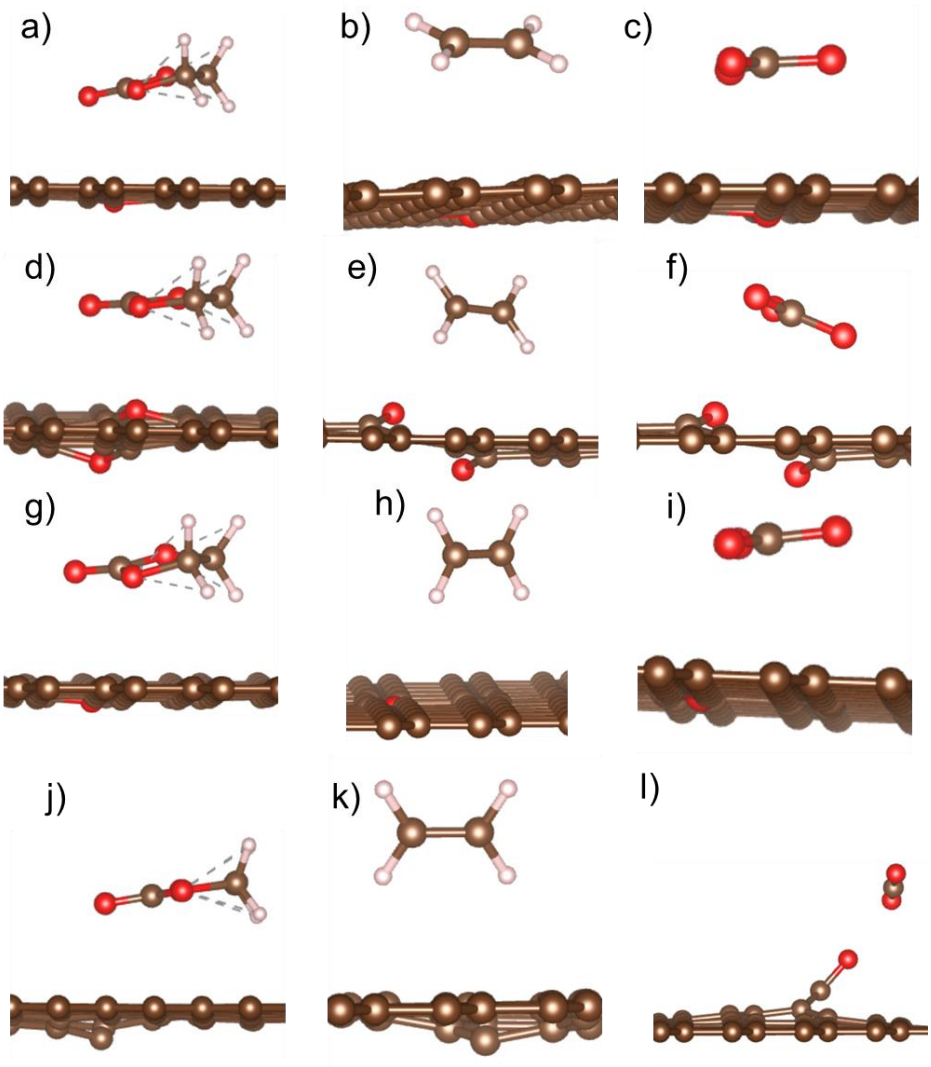

Figure S6. Zoomed in view of optimised structure for the basal plane models with a) EC, b) C_2H_4, and c) CO_3 on O_C defect, d) EC, e) C_2H_4, and f) CO_3 on $2O_C$ defect, g) EC, h) C_2H_4, and i) CO_3 on O_CV_C defect, j) EC, k) C_2H_4, and l) CO_3 on V_C defect (with CO_3 broken down forming a CO_2 molecule and a =O surface functional group). Brown spheres are carbon atoms, red oxygen, and white hydrogen.

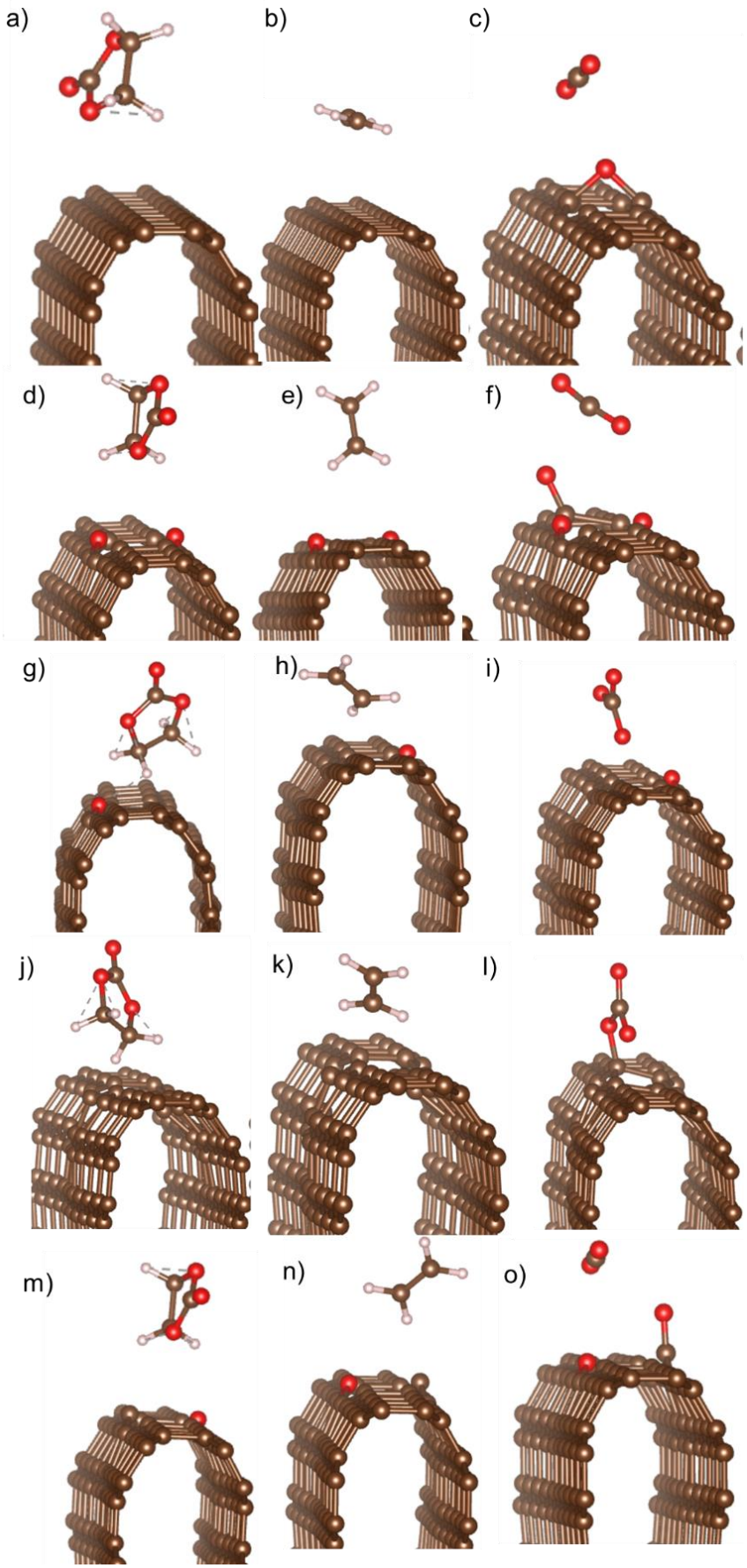
a)
b)
c)
d)
e)
f)
g)
h)
i)
j)
k)
l)
m)
n)
o)

Figure S7. Zoomed in view of optimised structure for the abrupt models (only one carbon surface shown) with a) EC, b) C_2H_4, and c) CO_3 on pristine surface (with CO_3 broken down forming a CO_2 molecule and a -O surface functional group), d) EC, e) C_2H_4, and f) CO_3 on $2O_C$ surface defect, g) EC, h) C_2H_4, and i) CO_3 on O_CV_C surface defect, j) EC, k) C_2H_4, and l) CO_3 on V_C surface defect, and m) EC, n) C_2H_4, and o) CO_3 on O_C surface defect (with CO_3 broken down forming a CO_2 molecule and a =O surface functional group). Brown spheres are carbon atoms, red oxygen, and white hydrogen.

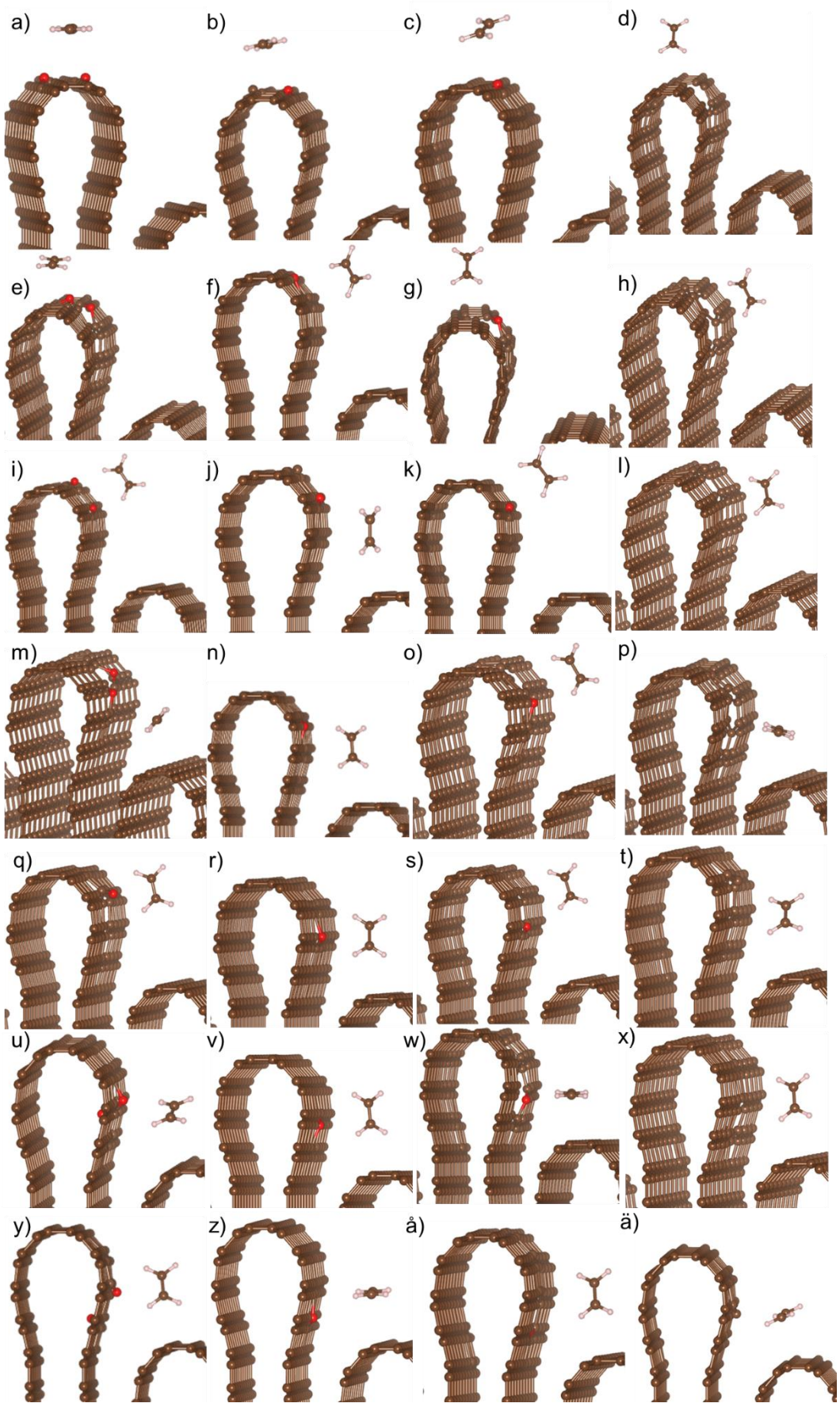
a)
b)
c)
d)
e)
f)
g)
h)
i)
j)
k)
l)
m)
n)
o)
p)
q)
r)
s)
t)
u)
v)
w)
x)
y)
z)
å)
ä)

Figure S8. Zoomed in view of optimised structure for the rough models with C_2H_4 at defect sites (nomeclature for defect sites is given in Figure 1b in the main paper). Row one shows C_2H_4 at site P1 with a) $2O_C$ defect, b) O_C defect, c) O_CV_C defect, and d) V_C defect. Row two shows C_2H_4 at site P2 with e) $2O_C$ defect, f) O_C defect, g) O_CV_C defect, and h) V_C defect. Row three shows C_2H_4 at site P3 with i) $2O_C$ defect, j) O_C defect, k) O_CV_C defect, and l) V_C defect. Row four shows C_2H_4 at site P4 with m) $2O_C$ defect, n) O_C defect, o) O_CV_C defect, and p) V_C defect. Row five shows C_2H_4 at site P5 with q) $2O_C$ defect, r) O_C defect, s) O_CV_C defect, and t) V_C defect. Row six shows C_2H_4 at site P6 with u) $2O_C$ defect, v) O_C defect, w) O_CV_C defect, and x) V_C defect. Row seven shows C_2H_4 at site P7 with y) $2O_C$ defect, z) O_C defect, å) O_CV_C defect, and ä) V_C defect. Brown spheres are carbon atoms, red oxygen, and white hydrogen.

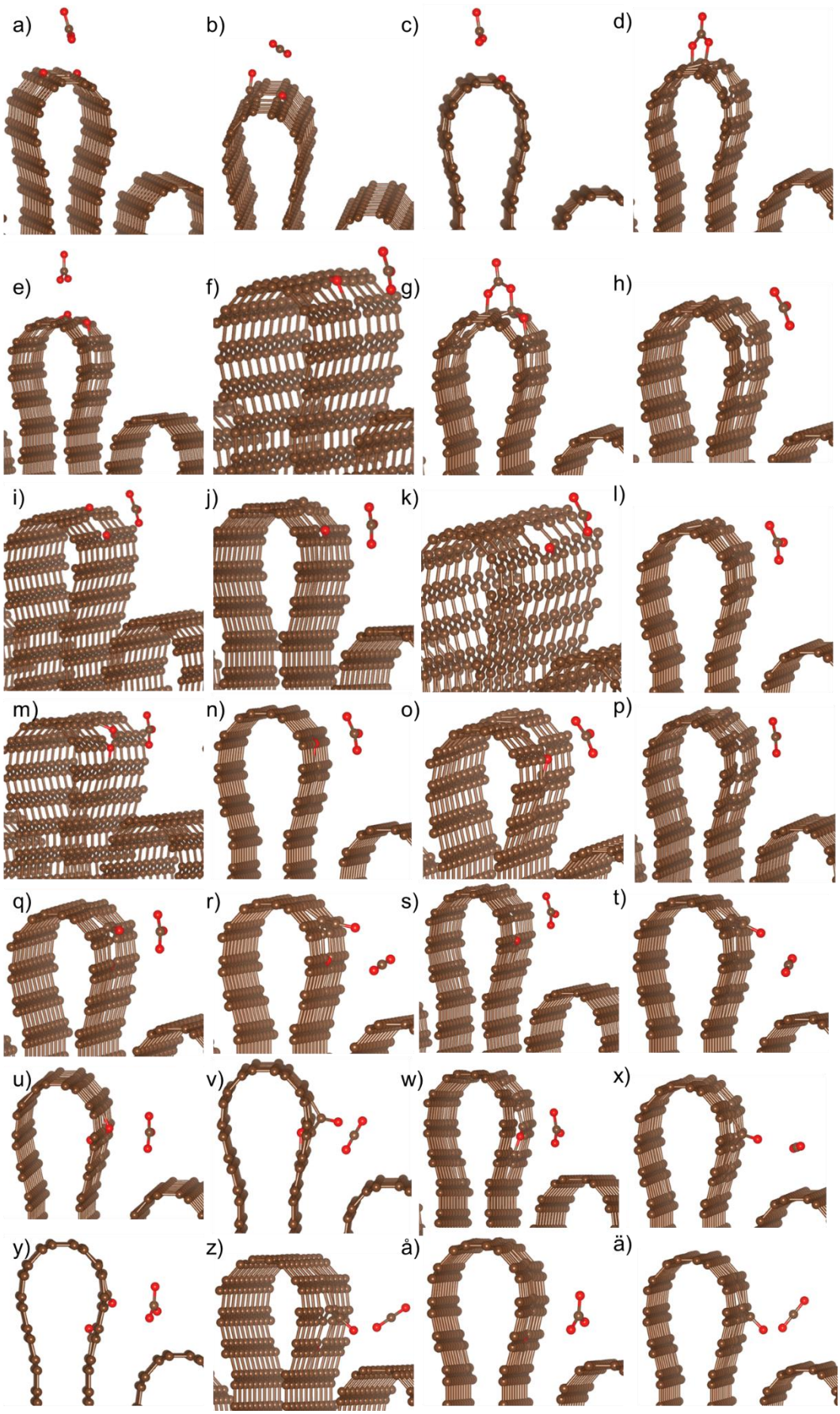
a)
b)
c)
d)
e)
f)
g)
h)
i)
j)
k)
l)
m)
n)
o)
p)
q)
r)
s)
t)
u)
v)
w)
x)
y)
z)
å)
ä)

Figure S9. Zoomed in view of optimised structure for the rough models with CO_3 at defect sites (nomeclature for defect sites is given in Figure 1b in the main paper). Row one shows CO_3 at site P1 with a) $2O_C$ defect, b) O_C defect (with CO_3 broken down forming a CO_2 molecule and a =O surface functional group), c) O_CV_C defect, and d) V_C defect. Row two shows CO_3 at site P2 with e) $2O_C$ defect, f) O_C defect, g) O_CV_C defect, and h) V_C defect. Row three shows CO_3 at site P3 with i) $2O_C$ defect, j) O_C defect, k) O_CV_C defect, and l) V_C defect. Row four shows CO_3 at site P4 with m) $2O_C$ defect, n) O_C defect, o) O_CV_C defect, and p) V_C defect. Row five shows CO_3 at site P5 with q) $2O_C$ defect, r) O_C defect (with CO_3 broken down forming a CO_2 molecule and a =O surface functional group), s) O_CV_C defect, and t) V_C defect (with CO_3 broken down forming a CO_2 molecule and a =O surface functional group). Row six shows CO_3 at s ite P6 with u) $2O_C$ defect, v) O_C defect (with CO_3 broken down forming a CO_2 molecule and a =O surface functional group), w) O_CV_C defect, and x) V_C defect (with CO_3 broken down forming a CO_2 molecule and a =O surface functional group). Row seven shows CO_3 at site P7 with y) $2O_C$ defect, z) O_C defect (with CO_3 broken down forming a CO_2 molecule and a =O surface functional group), å) O_CV_C defect, and ä) V_C defect (with CO_3 broken down forming a CO_2 molecule and a =O surface functional group). Brown spheres are carbon atoms, red oxygen, and white hydrogen.

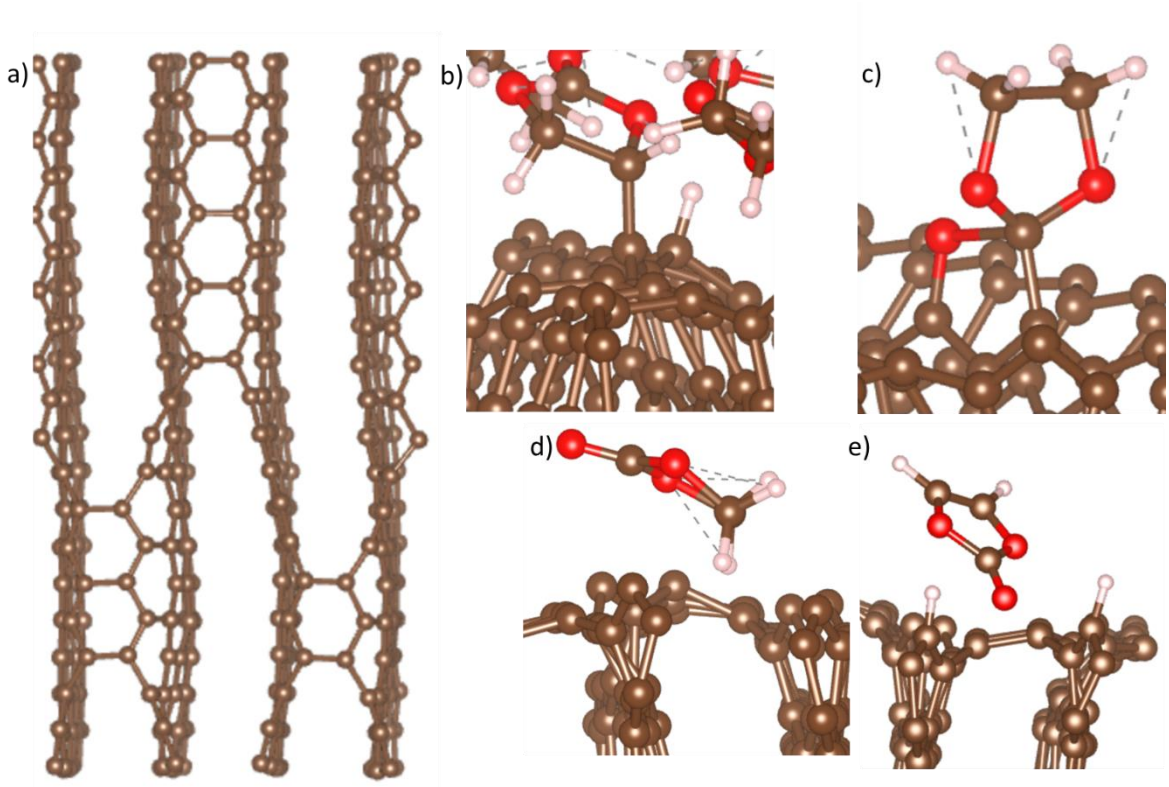

Figure S10. Zoomed in views of the features shown in Figure 7. a) Disordered carbon surface (top view) used for disordered carbon surface EC AIMD simulations. b) shows hydrogen abstraction from an EC molecule at 3.82 ps after equilibration, c) oxygen loss from EC to carbon surface at 6.84 ps after equilibration, d) EC interaction with surface at 25 ps after equilibration, and e) formation of vinylene carbonate through H loss to the disordered surface at 13.54 ps after equilibration.

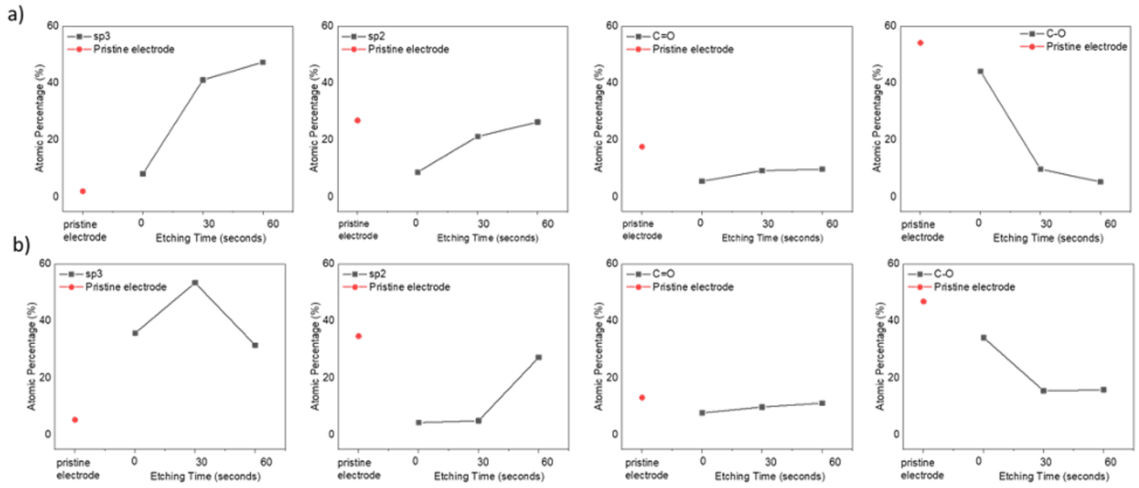

Figure S11. The atomic fractions calculated from the C1s spectra of a) ST1000 and b) ST1500 hard carbon anode cycled in 1M $NaPF_6$ in EC. (x=0), after 30 seconds of etching (x=30), after 60 seconds of etching (x=60).

Table S1. The atomic fractions and error margins calculated from the C1s and O1s spectra for ST1000.

	C 1s					O1s		
ST1000	sp^3	sp^2	C-O	C=O	$NaCO_3$	C-O	C=O	Na kll
Pristine electrode	2 (±0.1)	26.86 (±0.8)	54.15 (±1)	17.64 (±0.8)	-	61.29 (±1)	28.72 (±0.5)	9.99 (±0.3)
0 s	8.15 (±0.5)	8.73 (±1)	44.16 (±0.7)	5.54 (±0.3)	33.42 (±0.8)	26.04 (±0.5)	60.57 (±0.8)	13.39 (±0.5)
30 s	41.13 (±1)	21.26 (±0.8)	9.76 (±0.4)	9.24 (±0.5)	18.61 (±0.3)	14.76 (±0.5)	58.53 (±1)	26.61 (±0.8)
60 s	47.33 (±1)	26.3 (±0.8)	5.3 (±0.3)	9.73 (±0.6)	11.34 (±0.5)	12.25 (±0.3)	58.91 (±1)	28.83 (±0.8)

Table S2. The atomic fractions and error margins calculated from the C1s and O1s spectra for ST1500.

	C 1s					O1s		
ST1500	sp^3	sp^2	C-O	C=O	$NaCO_3$	C-O	C=O	Na kll
Pristine electrode	5.35 (±0.1)	34.7 (±1)	46.83 (±1)	13.12 (±0.4)	-	60.41 (±1)	29.5 (±1)	10.09 (±0.7)
0 s	35.73 (±1)	4.41 (±0.9)	34.15 (±0.8)	7.81 (±0.3)	17.9 (±0.5)	26.9 (±0.4)	57.65 (±1)	15.45 (±0.7)
30 s	53.38 (±1)	5.04 (±0.1)	15.52 (±0.5)	9.82 (±0.5)	16.25 (±0.5)	16.96 (±0.5)	52.21 (±1)	29.83 (±0.9)
60 s	31.55 (±0.8)	27.23 (±0.5)	15.87 (±0.5)	11.16 (±0.5)	14.08 (±0.4)	15.8 (±0.5)	51.54 (±1)	32.66 (±0.7)